

TITLE: ENHANCED ENERGY DEPOSITION SYMMETRY BY HOT ELECTRON TRANSPORT

AUTHOR(S): D. Wilson, J. Mack, E. Stover, D. VanHulsteyn, G. McCall,
and A. Hauer

MASTER

SUBMITTED TO: "Symmetry Aspects of Inertial Fusion Implosions
Topical Conference," Dr. Stephen Bodner,
Naval Research Laboratory, Washington, D.C. 20375



By acceptance of this article, the publisher recognizes that the U.S. Government retains a nonexclusive, royalty free license to publish or reproduce the published form of this contribution, or to allow others to do so, for U.S. Government purposes.

The Los Alamos Scientific Laboratory requests that the publisher identify this article as work performed under the auspices of the U.S. Department of Energy.

DISTRIBUTION OF THIS DOCUMENT IS UNLIMITED

UNIVERSITY OF CALIFORNIA



LOS ALAMOS SCIENTIFIC LABORATORY

Post Office Box 1663 Los Alamos, New Mexico 87545

An Affirmative Action/Equal Opportunity Employer



ENHANCED ENERGY DEPOSITION SYMMETRY BY HOT
ELECTRON TRANSPORT

D. Wilson, J. Mack, E. Stover, D. VanHulsteyn,
G. McCall, and A. Hauer

LOS ALAMOS NATIONAL LABORATORY

High energy electrons produced by resonance absorption carry the CO₂ laser energy absorbed in a laser fusion pellet. Since a symmetric implosion is crucial to obtain high DT densities, the definition of techniques to obtain symmetric energy deposition is important. One of these, symmetric laser illumination of the pellet surface, is discussed in other papers at this conference. This paper addresses the additional symmetrization that can be achieved by lateral transport of the hot (suprathermal) electrons as they deposit their energy.

This paper is divided into two parts. First, a K_α experiment will be discussed that, although designed for a different purpose, shows a surprising symmetrization of energy deposition achieved by adding a thin layer of plastic to a copper sphere. Second, our efforts to numerically model this effect will be discussed.

The emission of K_α radiation can be used to diagnose suprathermal electron transport. In the K_α radiation process, a high energy electron collides with and ejects an atomic electron from the K shell. In the subsequent decay of an outer shell electron into the K shell, a K_α, or K_β, etc. photon is emitted. In our experiment, a 250 μm diameter copper sphere is the source of K_α emission. A 75 μm layer of plastic (CH) was added to investigate the transport of

suprathermal electrons. An additional 3 μm nickel coating was added to a few targets to identify the spatial extent of the laser spots.

These targets were illuminated by between 2 and 7 focussed beams from the 8 beam HELIOS laser. The typical CO_2 laser pulse had a full width at half maximum of 0.7 ns with a 10 to 90% rise time of 0.24 ns and a 90 to 10% decay time of 1.1 ns. The laser spot diameter was estimated to be about 100 μm with a peak intensity of about 10^{16} w/cm^2 . Suprathermal electron temperatures derived from the fastest ion velocity varied from 70 to 100 keV. Spatial extent of the suprathermal electron energy deposition was measured by an x-ray pinhole camera with a 100 μm diameter pinhole and a 25 μm nickel filter. Another pinhole camera with a cobalt filter that does not transmit copper K_{α} radiation verified that most of the signal recorded by the nickel filtered camera was due to K_{α} radiation rather than bremsstrahlung radiation produced by the suprathermal electrons.

Figure 1 is a reproduction of the pinhole image of a copper sphere coated with both CH and nickel. The observed emission is dominated by the K_{α} radiation emitted from the outer nickel layer. The pinhole camera is viewing this 6 beam shot from above at an angle of 30 degrees relative to the normal passing through the top beam spot. Observe that the radiation is strongly localized to the laser spots. In Fig. 2 only 2 laser beams are incident on a bare copper sphere. Again note that the emission is concentrated at the laser spots. In Fig. 3 however, a weakly emitting 75 μm thick plastic layer has been added, therefore essentially all of the emission comes from the copper sphere. Observe that the radiation emission is now symmetric. In this 7 beam shot three of the top four beams were present. It is this symmetrization effect that we attempt to understand.

Figure 4 displays the calibrated emission from images of the bare copper sphere (Fig. 2) and the plastic coated sphere (Fig. 3). Film density has been converted to emission in units of copper K_{α} photons per μm^2 across a diameter as seen by the pinhole camera. In both cases the diameter passes through the center of the laser spot.

Our numerical calculations of this experiment use results from both LASNEX, which models both hydrodynamic motion and suprathreshold electron diffusion, and ACCEPT,¹ a three-dimensional (3-D) Monte Carlo electron/photon transport code. Since suprathreshold electrons are created at the critical surface for 10.6 μm light and transport into the copper sphere to create K_{α} radiation, the location of the critical surface will be crucial to suprathreshold electron transport. Because combined calculations of two-dimensional (2-D) hydrodynamics and suprathreshold electron transport are prohibitively long, we have chosen to model the experiment first with one-dimensional (1-D) hydrodynamic calculations and then, in a static geometry, study the 2-D suprathreshold electron transport and the attendant electron/photon cascade including both K x-ray and bremsstrahlung production and transport.

Since suprathreshold electrons lose their energy and create K_{α} radiation on a time scale that is short compared to the duration of the laser pulse, we have modeled the radial density profile at 0.7 ns, the midpoint of laser pulse. At this time the critical surface has expanded to a radius of 410 μm in the plastic coated target and to 320 μm in the bare copper target. The LASNEX calculated radial density profile for the plastic coated target is presented in Fig. 5.

1. J. A. Halbleib, "ACCEPT: A Three-Dimensional Electron/Photon Monte Carlo Transport Code Using Combinatorial Geometry," Sandia National Laboratory, SAND-79-0415, May 1979.

This profile was approximated by the dashed profile and used by ACCEPT in the 2-D geometry shown schematically in Fig. 6.

In the ACCEPT calculations we have assumed that the laser strikes only the annular section of the geometry which is located along the symmetry axis. This is consistent with the 100 μm diameter laser spot at tightest focus. The absorbed laser energy is then converted into electrons with a distribution in energy of a 1-D Maxwellian directed inward with a uniform hemispherical distribution. This isotropic distribution should give rise to more symmetrization than a monodirectional source directed radially inward and thus provide a conservative approach to the choice of the source distribution.

The pinhole camera observations were simulated by integrating the energy distribution in the copper sphere predicted by ACCEPT to one optical depth (25 μm at $\rho = 8.9 \text{ g/cm}^3$) along lines-of-sight emanating from an arc as seen by the camera. This approximation was convenient for the present work. The K_{α} emission was assumed to be proportional to the energy deposition. This is a justifiable approximation that will be relaxed in future studies where K_{α} emission and transport will be tallied explicitly.

ACCEPT results are compared in Fig. 7 with the observed emission for the bare copper sphere case. The number of suprathermal electrons introduced into each Monte Carlo problem was chosen to yield acceptable uncertainty statistics. An absolute magnitude for the K_{α} emission could not be obtained from our simple calculations, therefore both experimental and numerical results are normalized for presentation. Note that the relative calculated and observed intensities agree quite well.

Poor agreement between calculated (ACCEPT) and observed intensity can be seen in Fig. 8 when the 75 μm plastic layer is added. The observed symmetrization is not predicted. In fact the electrons produce the same energy

deposition asymmetry when the calculation is repeated in the same geometry assuming no interaction with the plastic. The electrons behave as if the plastic is transparent to scattering interactions (e.g. electrons still deposit energy in the plastic). We are unable to explain the symmetrization of energy deposition caused by the 75 μm thick plastic layer.

Outward motion of the critical surface was observed to enhance symmetry in our Monte Carlo simulations. The critical surface of the plastic coated target however, would have had to move much farther than the bare copper sphere target critical surface. Our 1-D hydrodynamic calculations show that the differential expansion of the critical surface was not large enough to account for the measured difference in symmetry.

Varying the suprathreshold electron temperature from 50 keV to 200 keV produced no substantial change in symmetrization. Return current electric fields are probably not the cause either. They should inhibit rather than enhance lateral transport. Increasing the electron-ion scattering cross-section by a factor of 10 in a 2-D LASNEX diffusion calculation showed little enhancement.

Clearly a better experiment should be performed and improvements in theory need to be made. In a future experiment, a single laser beam with varying peak intensity should be used so that multibeam effects can be eliminated and the suprathreshold electron temperature can be varied. The plastic layer thickness should be varied so that the transition between bare copper asymmetry and full symmetry can be examined in greater detail. Critical surface motion should be measured as well as the suprathreshold electron generated bremsstrahlung spectrum from which the suprathreshold electron temperature can be inferred.

When modeling this experiment, both K_{α} emission and transport, not just the energy deposition should be tallied. Variations in the ACCEPT code scattering cross-sections should be explored as well as combined Monte Carlo suprathemal electron transport and hydrodynamics calculations. We hope that these improvements in experiment and modeling will improve our understanding of this interesting and important effect.

FIGURE 1. PINHOLE IMAGE OF A 250 MICRON
DIAMETER COPPER SPHERE COATED WITH A
75 MICRON PLASTIC LAYER AND A 3 MICRON
NICKEL LAYER

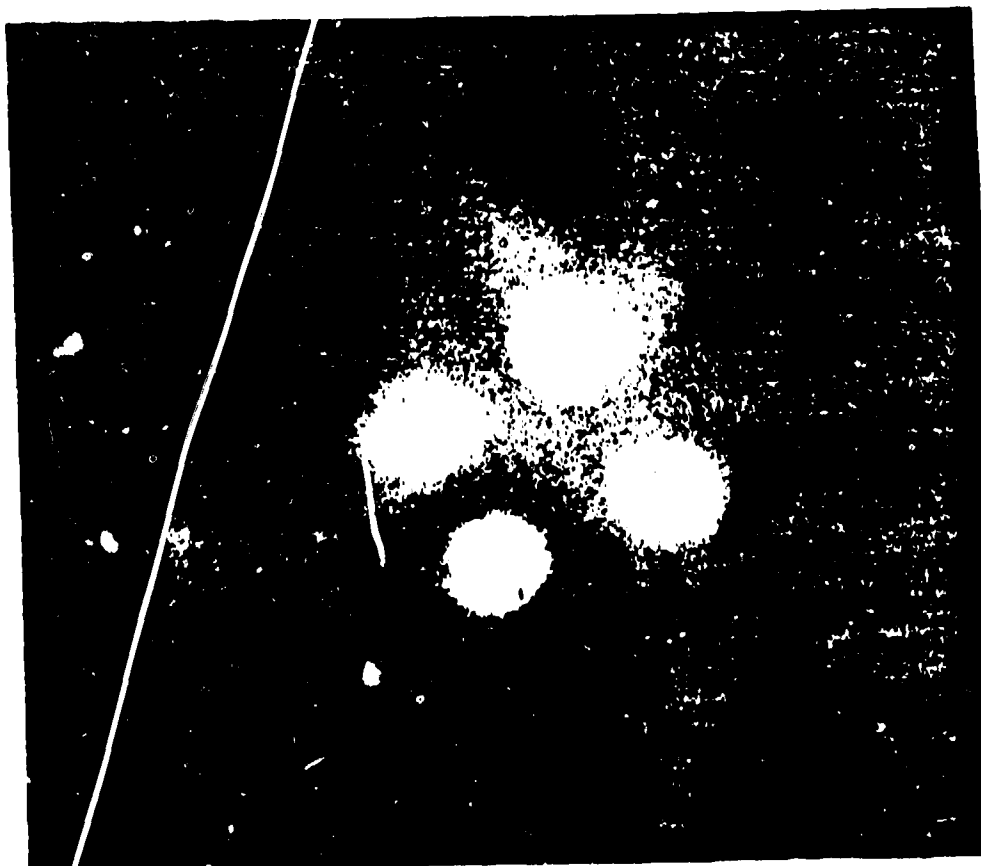


FIGURE 2. PINHOLE IMAGE OF A 250 MICRON
DIAMETER BARE COPPER SPHERE

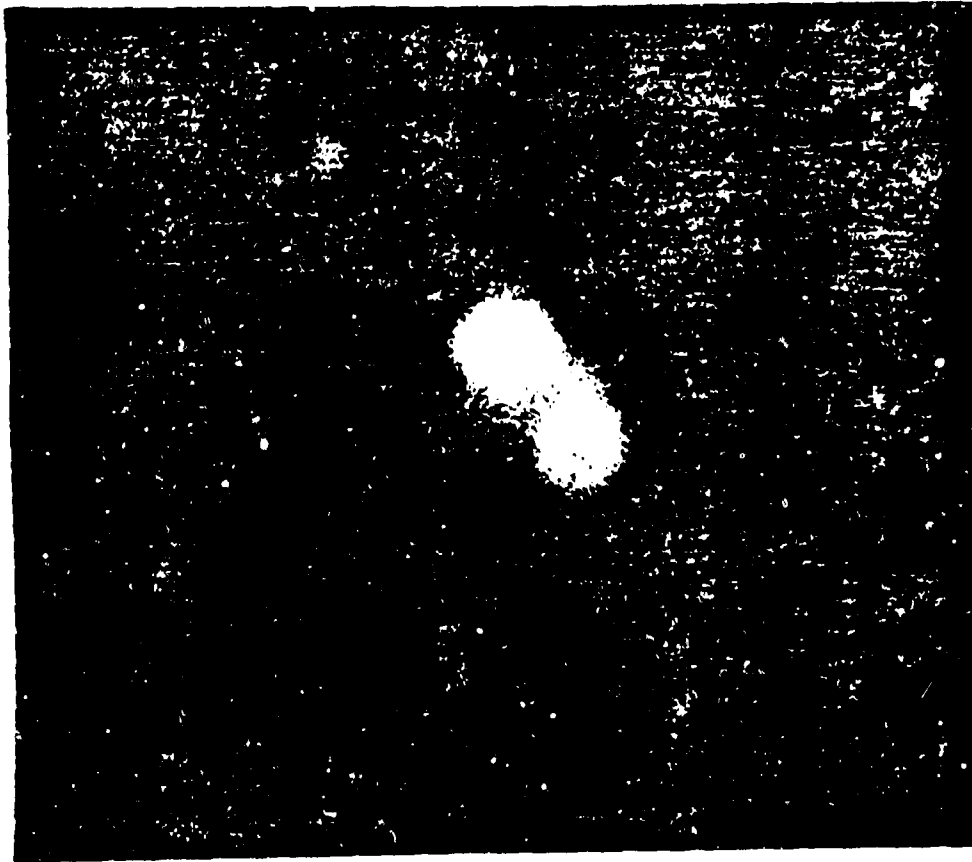


FIGURE 3. PINHOLE IMAGE OF A 250 MICRON
DIAMETER COPPER SPHERE COATED WITH A
75 MICRON LAYER OF PLASTIC

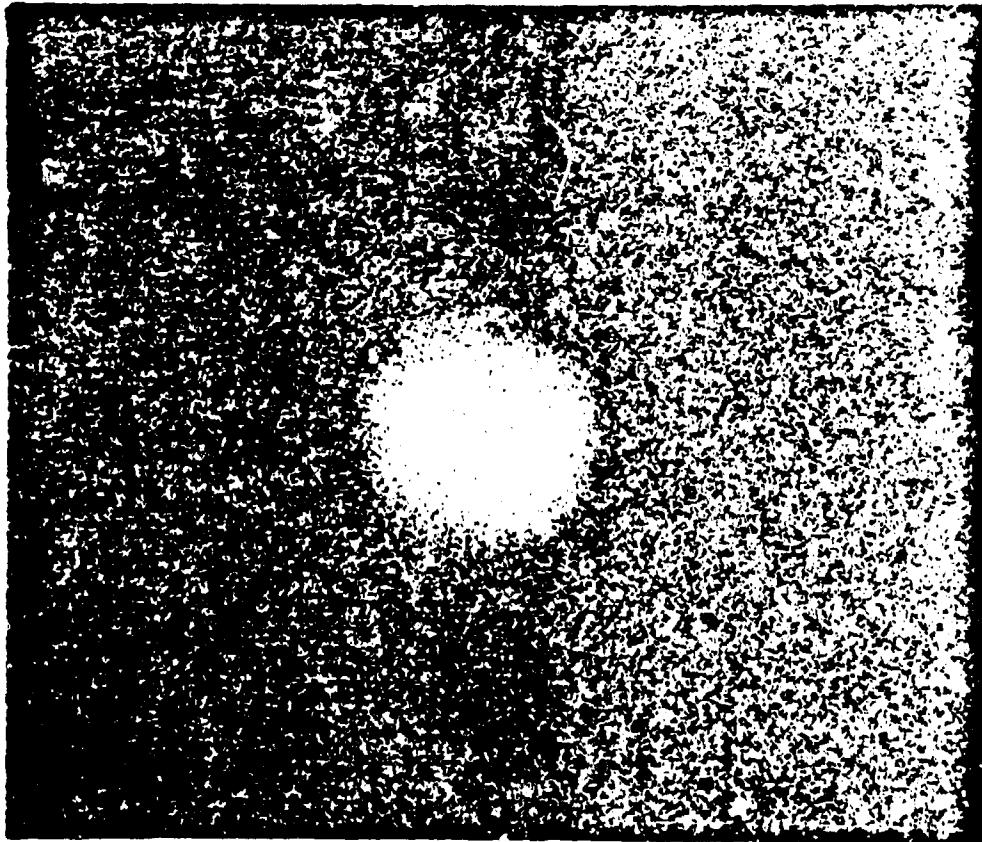


FIGURE 4. CALIBRATED EMISSION FROM IMAGES OF THE BARE COPPER SPHERE AND THE PLASTIC COATED SPHERE

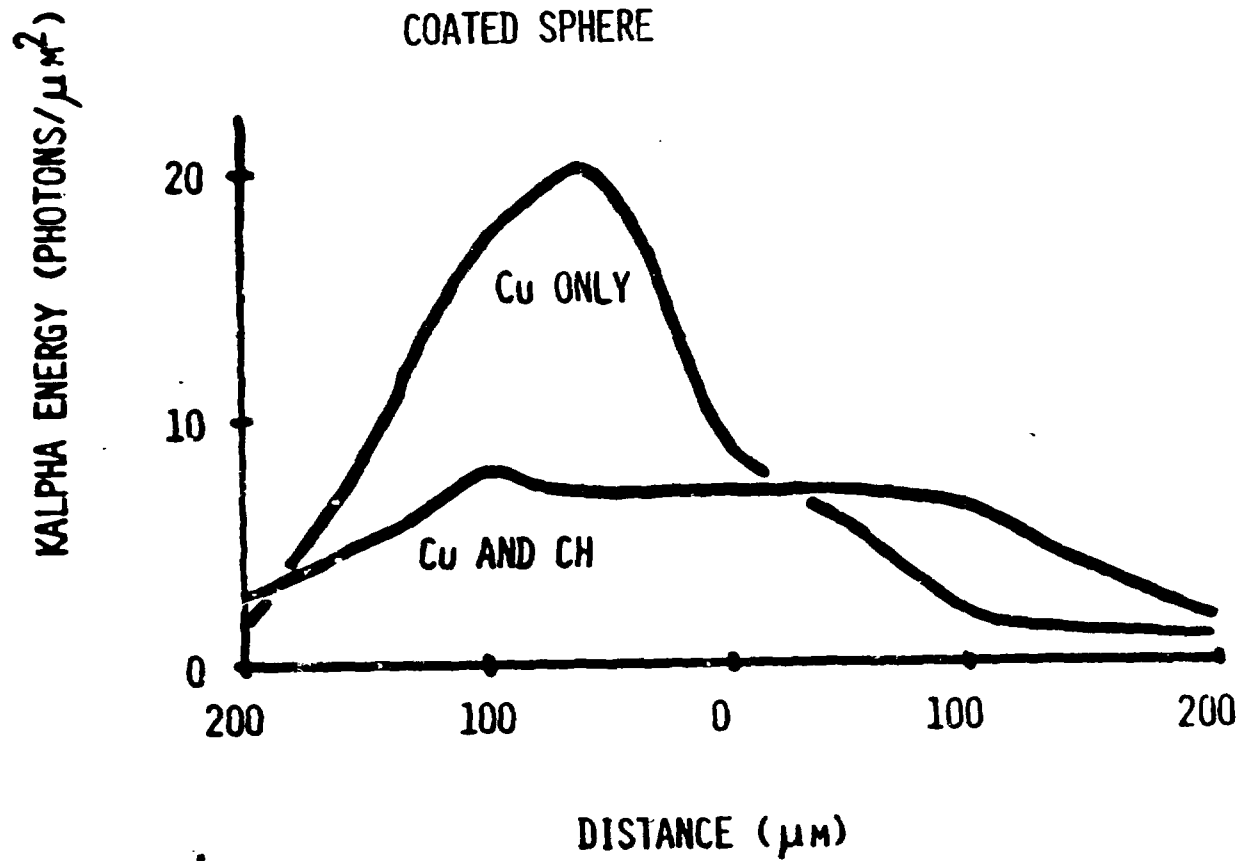


FIGURE 5. RADIAL DENSITY PROFILES CALCULATED BY 1-D LASNEX AND USED BY ACCEPT FOR PLASTIC COATED TARGETS

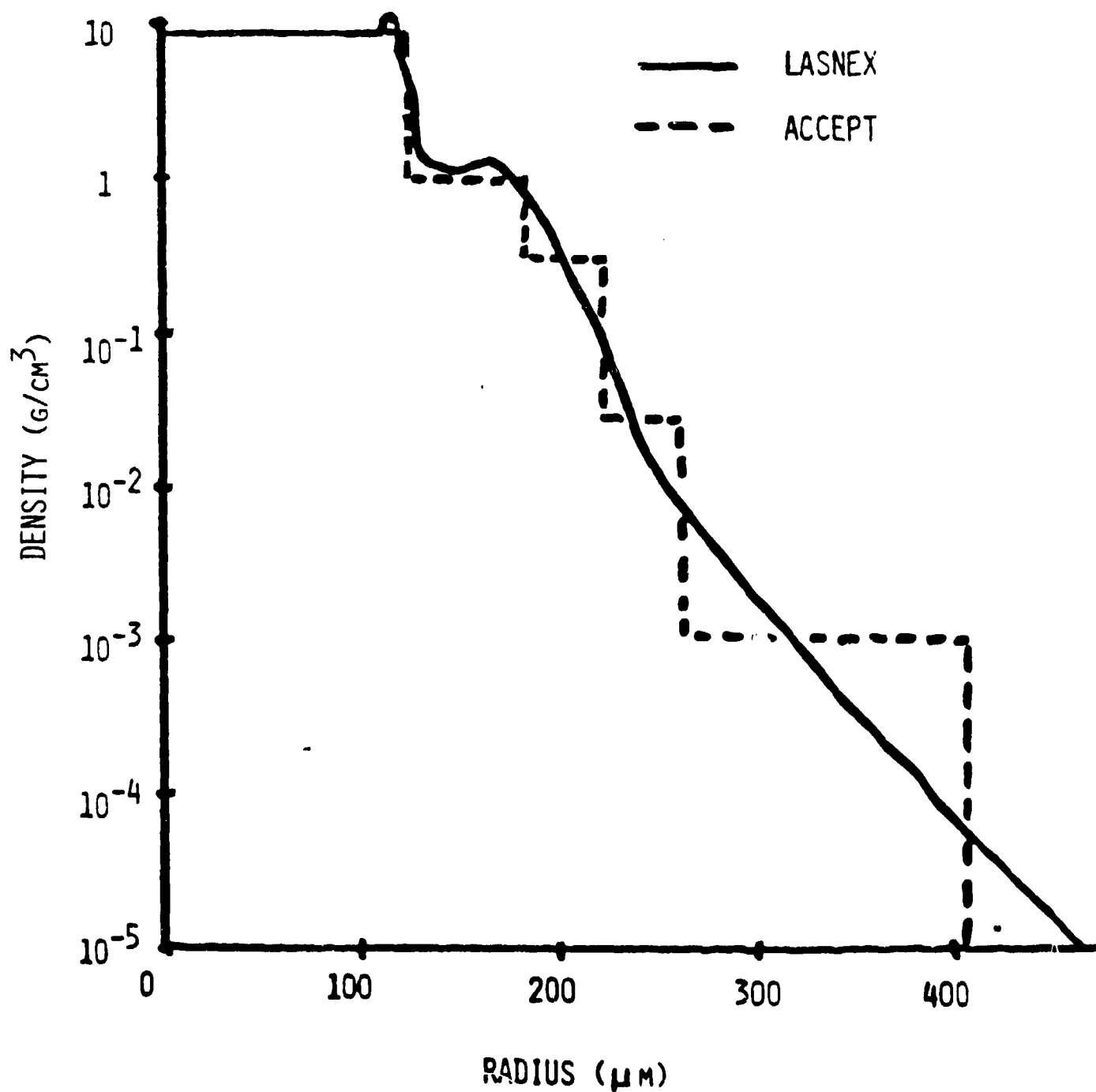


FIGURE 6. ACCEPT/LASNEX 2-D GEOMETRY

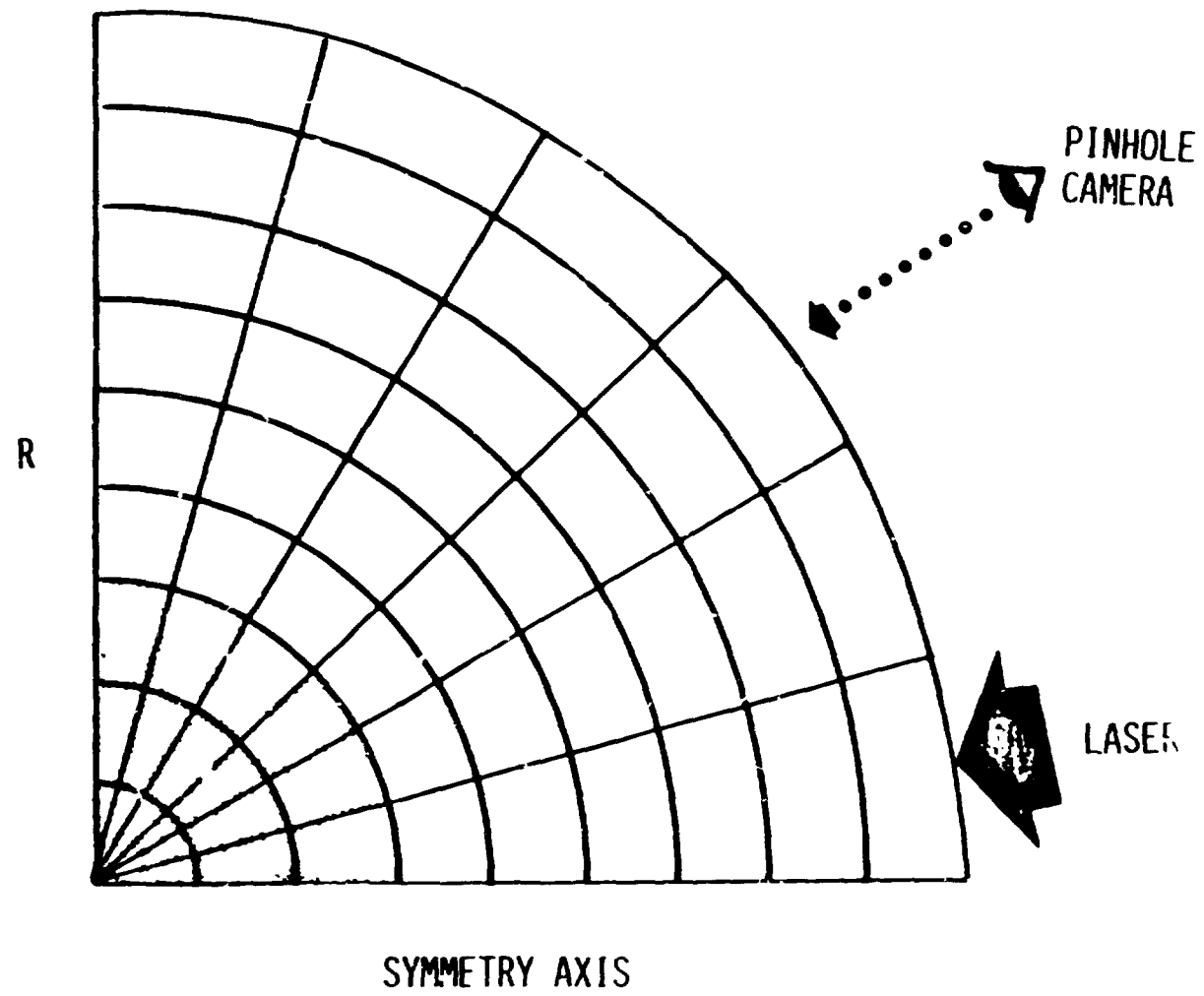


FIGURE 7. COMPARISON OF ACCEPT RESULTS
WITH OBSERVED EMISSION FOR THE BARE
COPPER SPHERE

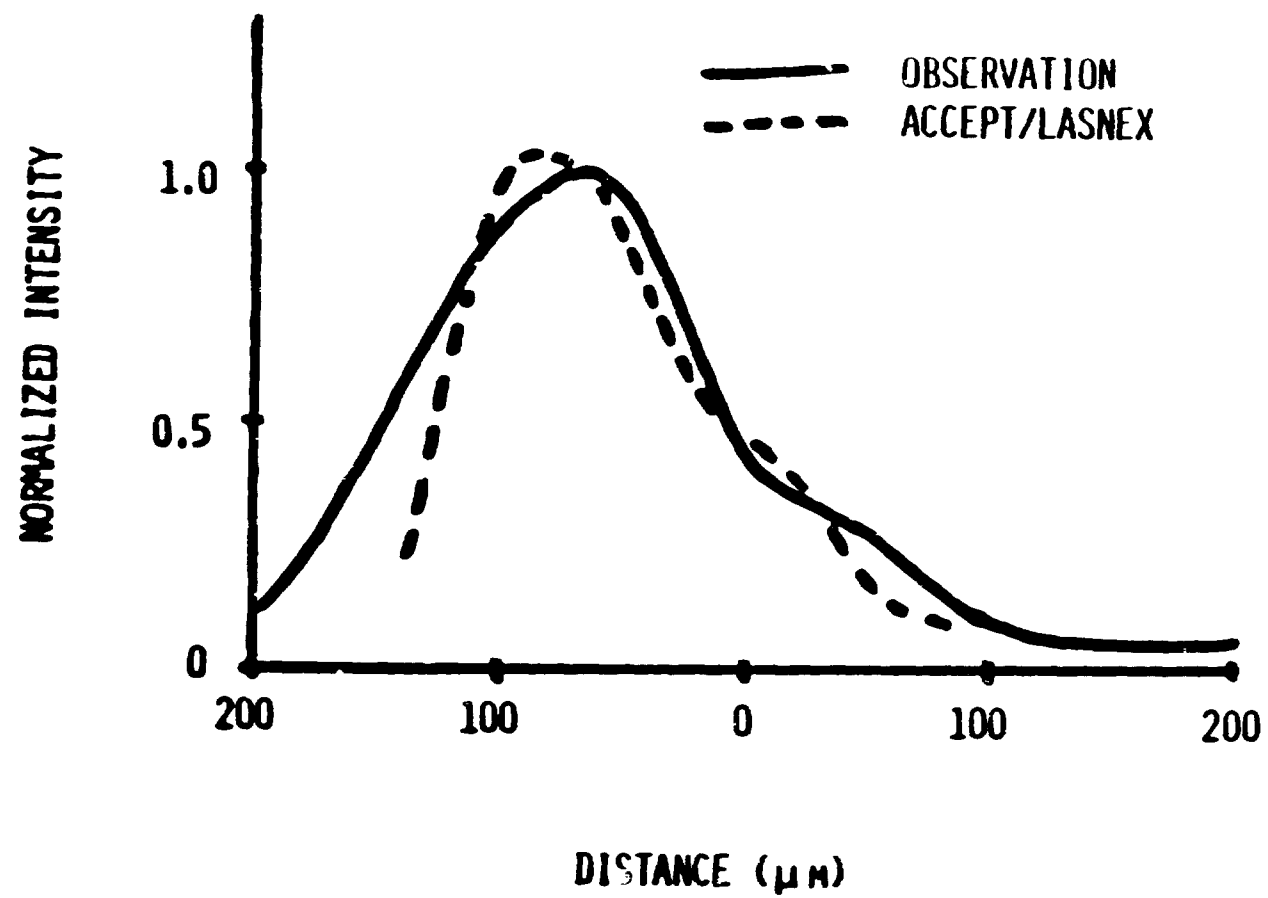


FIGURE 8. COMPARISON OF ACCEPT RESULTS WITH OBSERVED EMISSION FOR THE PLASTIC COATED COPPER SPHERE

